Histol Histopathol (2017) 32: 1041-1055

http://www.hh.um.es

Histology and Histopathology

From Cell Biology to Tissue Engineering

Seven days post-injury fate and effects of genetically labelled adipose-derived mesenchymal cells on a rat traumatic brain injury experimental model

Ioanna Dori[1], Spyros Petrakis[2]*, Aggeliki Giannakopoulou[1], Chryssa Bekiari[1], Ioannis Grivas[1], Evangelia K. Siska[2], Georgios Koliakos[2,3] and Georgios C. Papadopoulos[1]

[1]Laboratory of Anatomy, Histology and Embryology, School of Veterinary Medicine, Faculty of Health Sciences, Aristotle University of Thessaloniki, and [2]Biohellenika, Pylaia and [3]Department of Biochemistry, School of Medicine, Faculty of Health Sciences, Aristotle University of Thessaloniki, Thessaloniki, Greece

*Current address: Institute of Applied Biosciences (INAB), Centre for Research and Technology Hellas (CERTH), Thessaloniki, Greece

Summary. Mesenchymal stromal cells (MSC) have been suggested to have beneficial effects on animal models of traumatic brain injury (TBI), owing to their neurotrophic and immunomodulatory properties. Adipose tissue-derived stromal cells (ASCs) are multipotent MSC that can be harvested with minimally invasive methods, show a high proliferative capacity, low immunogenicity if allogeneic, and can be used in autologous or heterologous settings. In the present study ASCs were genetically labelled using the Sleeping Beauty transposon to express the fluorescent protein Venus. Venus+ASCs were transplanted intra-cerebro-ventricularly (ICV), on a rat TBI model and their survival, fate and effects on host brain responses were examined at seven days post-injury (7dPI). We provide evidence that Venus+ASCs survived, migrated into the periventricular striatum and were negative for neuronal or glial lineage differentiation markers. Venus+ASCs stimulated the proliferation of endogenous neural stem cells (NSCs) in the brain neurogenic niches, the subventricular zone (SVZ) and the hippocampal dentate gyrus (DG). It was also evident that Venus+ASCs modify the host brain's cellular microenvironment both at the injury site and at their localization area by promoting a significant reduction of the lesion area, as well as altering the post-injury, pro-inflammatory profile of microglial and astrocytic cell populations. Our data support the view that ICV transplantation of ASCs induces alterations in the host brain's cellular response to injury that may be correlated to a reversal from a detrimental to a beneficial state which is permissive for regeneration and repair.

Key words: Mesenchymal cell transplantations, Traumatic brain injury

Offprint requests to: Professor Georgios C. Papadopoulos, DVM, PhD, Laboratory of Anatomy, Histology and Embryology, Faculty of Veterinary Medicine, School of Health Sciences, Aristotle University of Thessaloniki, 54124 Thessaloniki, Greece. e-mail: gpapadop@vet.auth.gr

DOI: 10.14670/HH-11-864

Introduction

Brain damage, produced by TBI, is a major cause of mortality and lifelong neurological deficits with high socioeconomic burden. To date, there is no effective treatment for neural repair, as current therapies aim at ameliorating the effects of secondary insult rather than repairing the primary tissue damage.

TBI can be induced by various factors, resulting in focal or diffuse injury. The primary insult involves massive cell death which in turn induces inflammation and reactive astrogliosis, mediated by the activation of local resident microglia and astrocytes as well as the recruitment of peripheral immune cells in this area, due to the disruption of the blood-brain barrier. These cells are key mediators of the brain's cellular responses to

injury through multiple interactions that are involved in regulation of neuroinflammation, neuroprotection and synaptic remodelling (Burda and Sofroniew, 2014; Loane and Kumar, 2016). The concept of stimulus-induced polarization of glial cells from a classical pro-inflammatory M1 to an alternative anti-inflammatory M2 phenotype has recently gained insight (Franco and Fernández-Suárez, 2015; Kumar et al., 2016; Loane and Kumar, 2016). However, despite the bimodal beneficial and detrimental effects of the M1/M2 states at the acute post-injury phase, it was recently shown that the pro-inflammatory profile remains primed, contributes to chronic neuroinflammation and is associated with neurodegenerative disorders (Witcher et al., 2015).

Studies using adult animal models of cortical injury have shown that TBI stimulates cell proliferation in the SVZ and the hippocampal DG adult neurogenic niches that peak during the first week after injury, suggesting the implication of this process in regenerative mechanisms. Newborn cells migrate from the SVZ to the injury site and differentiate into neurons or glial cells. In the hippocampal DG, injury-induced cell proliferation results in the production and functional integration of granule neurons (Richardson et al., 2009; Kernie and Parent, 2010; Gennai et al., 2015; Villasana et al., 2015). However, the innate capacity of the brain for structural and functional restoration after severe TBI is limited due to the extensive cell loss and inflammatory environment at the injury site that hamper tissue repair. Experimental data suggest that the boosting of endogenous neurogenesis with the use of growth factors, drugs or various treatments is related to cognitive functional improvement (Sun, 2016). Therefore, the development of efficient approaches aiming at modulating endogenous brain stem-cell proliferation, migration, differentiation and homing, either directly or indirectly by monitoring the neurogenic microenvironment is a promising therapeutic strategy for TBI. Cell therapy studies have demonstrated the potential of MSC to restore brain function after TBI, mediated by the secretion of multiple factors that promote the production, survival, migration and differentiation of newborn neurons (Donega et al., 2013a; Teixeira et al., 2013; Salgado et al., 2015). The neuroprotective, anti-inflammatory and angiogenic role of MSC in brain injuries has also been documented (Constantin et al., 2009; Uccelli et al., 2011; Zhang et al., 2015).

ASCs are multipotent MSC originating from adipose tissue. They are considered advantageous compared to other cell types because they are easily harvested, isolated in large numbers from the adipose stromal vascular fraction, show a high proliferative capacity, rapid expansion *in vitro* without a loss of stemness, genetic stability in long-term culture and low immunogenicity. Owing to their low MHC-I expression and lack of MHC-II molecules, they are not rejected when administered in allogeneic settings. Several preclinical and clinical studies have evaluated the safety of ASCs with respect to side effects and tumorigenesis, as well as their efficacy and therapeutic potential (Gimble et al., 2010; Ra et al., 2011; Diez-Tejedor et al., 2016). Therefore ASCs are considered promising candidates for cell therapy in a wide range of disorders, including brain injury and neurodegenerative diseases. ASCs have been shown to ameliorate cortical damage, reduce hippocampal cell death, attenuate the neurological deficits and improve cognitive and motor functions after TBI and ischemic brain injury and reduce cerebral inflammation and degeneration after stroke (Tajiri et al., 2014a,b; Chung et al., 2015; Mastro-Martínez et al., 2015). The action of ASCs is mediated through the paracrine effects of their secretome, that consists of various secreted trophic and immunomodulatory factors, including nerve growth factor, glial derived neurotrophic factor, and brain derived neurotrophic factor, cytokines such as vascular endothelial growth factor, immuno-suppressive factors, granulocyte/macrophage colony-stimulating factor, hepatocyte growth factor and stromal derived factor 1 (Rehman et al., 2004; Yañez et al., 2006; Schäffler and Büchler, 2007; Murohara et al., 2009; Kalbermatten et al., 2011; Kapur and Katz, 2013; Jumabay and Boström, 2015).

In the present study we used the Sleeping Beauty transposon (Mates et al., 2009), a novel non-viral method to generate genetically-labelled rat ASCs that stably produced the fluorescent protein Venus+. We then performed an allogeneic ICV transplantation of Venus+ASCs on a rat TBI model that has been employed in our previous studies (Sophou et al., 2006; Mellios et al., 2009; Zacharaki et al., 2010). We evaluated the survival, migration, differentiation and effects of Venus+ASCs on host brain responses at 7dPI.

Materials and methods

Animals

Adult (90 day-old) male Wistar albino rats (n=20) inbred in the animal facility of the laboratory of Anatomy, Histology and Embryology, Faculty of Veterinary Medicine, Aristotle University of Thessaloniki, were used both for the isolation and the transplantation of ASCs. Animals were housed with a 12:12-h light/dark cycle, at 22±1°C with 60% humidity, pellet food, and water *ad libitum*. Experiments were carried out in accordance with the European Communities Council Directive 86/609/EEC, approved by the Veterinary Directorate of Thessaloniki and was in compliance with the guidelines of the Greek government and the Aristotle University Ethics committee.

Animals were randomly assigned to one of three experimental groups: 1) animals that were subjected to TBI and Venus+ASCs ICV transplantation (TBI+ASCs), n=8; 2) animals that were subjected to TBI and normal saline ICV infusion (TBI+saline), n=6; 3) animals that

were subjected only to Venus+ASCs ICV transplantation, without TBI (naive+ASCs), n=6.

Isolation of ASCs

ASCs were isolated as previously described (Karathanasis et al., 2013). In brief, the inguinal fat pad was excised and digested with 0.5 mg/ml collagenase type-1 (Sigma). Cell suspension was centrifuged for 10 min at 600g and the cellular pellet containing ASCs was grown in Dulbecco's modified Eagle medium supplemented with 5% fetal calf serum, penicillin (100 IU/ml) and streptomycin (100 μg/ml).

Flow cytometry

ASCs ($1x10^6$ cells) were stained with anti-rat CD44 FITC (clone: OX-49, cat. number: 550974) and anti-rat CD90 PE (clone: OX-7, cat. number: 551401) antibodies (BD Pharmigen) against mesenchymal stem cell markers and measured in a Cytomics FC500 flow cytometer (Beckman Coulter) using the CXP2.2 software. Unstained cells were used as negative controls.

Generation of Venus+ ASCs

ASCs at passage 2 ($2x10^5$ cells) were seeded in a 6-well tissue culture plate and transfected with 7.5 μg of Sleeping Beauty 100 x transposase and pT2 Venus-neo® transposon (1:9 ratio) using Xfect reagent (Clontech), as described previously (Petrakis et al., 2012). Venus+ ASCs cells were selected at day 7 post transfection and expanded with 100 μg/ml G418. Cells were observed in an Axiovert microscope equipped with an HBO 50 mercury lamp and reflectors with fluorescence filter sets. Image acquisition was performed with the Fluorescence Lite software module of AxioVision LE (Carl Zeiss).

Multilineage differentiation of Venus+ ASCs

For osteogenic or adipogenic differentiation, Venus +ASCs at passage 5 were grown to 90% confluency and cultured for 28 days either in StemPro® Osteogenesis or StemPro® Adipogenesis medium (Invitrogen). Differentiation of Venus+ASCs into osteocytes or adipocytes was identified by Alizarin Red or Oil Red staining, respectively.

Treatments

Induction of TBI

TBI was induced as described previously (Sophou et al., 2006; Mellios et al., 2009; Zacharaki et al., 2010). Briefly, stereotactic surgery was performed under deep anaesthesia (ketamine/xylazine, 50/5 mg/kg i.p). After a midline skin incision, a portion of the skull and the dura mater was removed and the cerebral cortex was exposed. A unilateral (right hemisphere) lesion of the cerebral cortex (Bregma, 4.0 mm posterior; midline, 4.0 mm lateral) was made by subpial aspiration using a blunt-tipped needle connected to a vacuum pump. After recovering from anesthesia, the animals were returned to their cages and their postoperative course was closely monitored.

ICV transplantation of Venus+ASCs

Immediately after TBI, allogeneic Venus+ASCs were ICV transplanted ipsilateral to the injury site. Cells were aseptically collected from the culture flasks, resuspended in phosphate- buffered saline (PBS) at a concentration of $5×10^5$/10 μl PBS and transplanted (5 μl of suspension), using a Hamilton syringe, at the coordinates: Bregma, 1.5 mm posterior; midline, 2 mm lateral, and depth, 4 mm.The infusion rate was 1 μl/minute and the needle was left in place for another 5 min. Control animals were infused with normal saline (5 μl). The scalp was sutured, animals were kept at 37°C until recovering from anaesthesia and their postoperative course was closely monitored. No animals died after surgery.

5- Bromo-2'-deoxyuridine (BrdU) injections

A BrdU-administration protocol was applied for the labelling of a sufficient number of dividing NSCs in the neurogenic niches within a 24-h period, without labelling the same cells twice (Cameron and Mckay, 2001; McDonald and Wojtowicz, 2005). BrdU (Sigma, St. Louis MO) was dissolved in 0.9% saline (20 mg/ml) and animals were injected (100 mg/kg/injection, i.p) at 48 and 60 h post-injury. The time point of the first injection was justified by the previously reported peak stage of injury-induced proliferation of endogenous neural stem cells in adult rat brains (Rice et al., 2003; Urrea et al., 2007).

Tissue preparation

At 7dPI, deeply anesthetized animals were transcardially perfused with PBS, followed by 4% paraformaldehyde in 0.1 M phosphate buffer (PB), pH 7.4. Brains were removed, postfixed for 2 h and transferred into PB. Consecutive coronal sections were cut at 50 μm using a Vibratome (Leica VT 1000S, Germany). Selected sections were either stained with the conventional histological techniques Nissl and Masson's trichrome staining (M TRI), or processed for single or double immunofluorescence.

Assessment of the cortical injury and evaluation of the lesion area

One in six Nissl-stained, consecutive sections, between the anterior and posterior edge of the cortical injury area, were used for the calculation of the lesion volume. The atlas of Paxinos and Watson (Paxinos and

Watson, 2013) as well as our earlier material were used as reference (Sophou et al., 2006; Mellios et al., 2009). The selected sections were examined with a Zeiss Axioplan II photomicroscope, under a ×20 objective. The area of the injury cavity was measured by the computer-assisted image analysis system Image Pro-Plus 6.3 software (media Cybernetics Inc., Rockville, USA) and its volume was calculated by the following formula: [(area of the injury cavity in each section) × 0.050] (cubic millimeters). The entire cortical injury volume (μm^3) per brain was then calculated by multiplying the sum of the injury cavity areas by sampling interval and expressed as a ratio of the ipsilateral hemisphere to the contralateral hemisphere.

Immunofluorescence

Following blocking with 5% normal goat serum (NGS) for 15 min, sections were incubated overnight at 4°C in a PBS solution containing 5% NGS, 0.1% Triton X-100 and one of the following antibodies: anti-doublecortin (DCX) (goat, 1:100; Santa Cruz Biotechnology, Inc. Texas, USA), anti- glial fibrillary acidic protein (GFAP) (rabbit, 1:1000; Dako, Carpinteria CA), anti- neuron-specific nuclear protein (NeuN) (rabbit, 1:800; Millipore, CA, USA), anti-ionized calcium binding adaptor molecule 1 (Iba1) (goat, 1:1000; Abcam, U.K), anti-Ki67 protein (mouse, 1:100; Millipore, CA USA), anti-calbindin D-28K (rabbit, 1:800; Millipore, CA, USA), anti-S100 protein (rabbit, 1:1000; Dako, Denmark), anti-von Willebrand factor (vWF) (rabbit, 1:300, Santa Cruz Biotechnology, Inc. Texas, USA) and anti-BrdU (mouse, 1:200; Dako, Denmark). Following washes in PBS, sections were incubated for 2 h in the dark at RT with the following secondary antibodies: Alexa Fluor 488 (goat anti-rabbit, 1:200; Invitrogen/Molecular Probes, Grand Island, NY, USA), Alexa Fluor 555 (goat anti-rabbit, goat anti-mouse, donkey anti-goat; 1:200; Invitrogen/Molecular Probes, Grand Island, NY, USA). Sections destined for BrdU immunolabelling were incubated in 4N HCl, at 37°C for 20 min, prior to blocking. After washes in PBS, they were processed for immunofluorescence as described above. Control sections, in which primary or secondary antibodies were omitted, were used as negative controls. Sections were coverslipped with prolong gold antifade reagent (Biotium) and examined with a Zeiss Axioplan II fluorescence microscope and a confocal laser microscope (CLSM; Nikon Eclipse C1; EZ - C1 3.20 software).

Localization and differentiation of Venus+ASCs

Equidistant sections (at least 10 per brain) along the rostro-caudal extent of the lateral ventricle (Bregma, +2.28mm anterior to -0.96mm posterior), including the periventricular striatal parenchyma, were collected and examined for the presence of Venus+ASCs. The proliferative ability of Venus+ASCs was assessed with immunofluorescence against Ki67 whilst their differentiation towards neuronal or glial lineages was evaluated with the use of the GFAP, DCX, NeuN, calbindin and S100 markers. Co-expression of the Venus signal with the above markers was examined under the CLSM in Z- stack captured images (1μm optical thickness per plane).

Quantitative analysis

Quantification of GFAP and Iba1 immunoreactivity on the cortical injury site and the periventricular striatal parenchyma

Quantitative assessment was performed by an investigator who was blinded to the experimental groups. The quantification of GFAP and Iba1 immunoreactivity on the cortical injury site and the periventricular striatal parenchyma was performed using the Image Pro-Plus 6.3 software (media Cybernetics Inc., Rockville, USA). From each brain, one in six consecutive sections, including the peri-injury area or the periventricular striatal parenchyma, was immunostained against GFAP or Iba1 and was captured with a digital camera (SSC-DC38P; SONY CHyper HAD), connected to a Zeiss Axioplan II fluorescence microscope (x20 objective). One constructed image was taken from each section and changed to an 8-bit image (turned to a black and white image). The peri-injury area or the periventricular striatal parenchyma was delimited and the percentage of illuminated pixels (white pixels) was calculated, following standard procedures. The mean percentage (% pixel area per optical field) was calculated per brain per marker of interest and the mean ±S.D. was estimated for each experimental group. In order to investigate whether differences in Iba1+ pixel area per optical field reflected differences in the total number of Iba1+ cells or alterations in their morphological features, we estimated the total number of Iba1+ cells in the peri-injury area in each experimental group. For this purpose, ten systematically selected sections through the injury area, or the corresponding cortical area of uninjured animals were selected from each brain and labelled for Iba1. In each section, the core-surrounding peri-injury area or the corresponding uninjured area was demarcated with the use of a digital camera (SSC-DC38P; SONY CHyper HAD) and appropriate software (Image Pro-Plus 6.3; media Cybernetics Inc., Rockville, USA). The number of Iba1+ cells was counted exhaustingly under a Zeiss Axioplan II fluorescence microscope (x40 objective) and was expressed as number of Iba1+ cells/mm^2 of demarcated area. The average number of Iba1+ cells/mm^2 was then estimated for each brain and the mean ± SD was calculated for each experimental group.

Quantification of BrdU⁺ cells in the neurogenic SVZ and DG

The total numbers of $BrdU^+$ cells per SVZ and

hippocampal DG was quantified using the modified fractionator method (Kronenberg et al., 2003; Bekiari et al., 2015). Briefly, in each brain, one in ten sections through the SVZ (Bregma, +2.28mm anterior to -0.96mm posterior; 6 - 7 sections per brain) and one in five sections through the hippocampal DG (Bregma, -2.56 to -4.16 mm posterior; 6 - 8 sections per brain) were collected and stained for BrdU. All immunoreactive cells were counted under a x40 objective (Zeiss Axioplan II fluorescence microscope) with the use of a SONY digital camera (SSC-DC38P; SONY CHyper HAD), blindly by the same observer. The total number of $BrdU^+$ cells per SVZ and DG (ipsilateral and contralateral) was defined as the sum of the $BrdU^+$ cells counted in the sampled sections multiplied by the inverse of the section sampling (x10 or x5 for the SVZ and the DG, respectively).

Statistical analysis

The data are reported as mean ± SD. Statistical analysis of the data was performed using the SPSS 20.0 statistical software. One-way ANOVA (Dunnett's and Bonferroni post-hoc tests) and independent samples T-test were used for comparisons between groups. Homogeneity of variances was tested using the Levene's test and when violated, the nonparametric two-tailed Kruskal-Wallis was assessed for multiple comparisons, followed by the Mann-Whitney U test (two-tailed) for two-by-two comparisons. Significance was set at $P<0.05$ and at $P<0.001$.

Results

Generation and characterization of Venus+ ASCs

Plastic-adherent ASCs with a fibroblastic morphology were isolated from rat adipose tissue and expanded *in vitro* (Fig. 1A). Cells displayed a high proliferation rate with a doubling time of approximately 48hrs. Phenotypic characterization showed that these cells were 99.6% double positive for CD44 and CD90 stem cell markers (Fig. 1B), verifying their mesenchymal origin. ASCs were genetically lebelled using the Sleeping Beauty transposon system. Cells were transfected with a bicistronic transposon plasmid encoding Venus fluorescent and neo^R antibiotic resistance proteins (Fig. 1C) in the presence of hyperactive transposase Sleeping Beauty 100X. Selection with G418 antibiotic resulted in the generation of a homogeneous fluorescent ASC population, which expressed the Venus signal for several passages (Fig. 1D). Next, we investigated whether Venus+ ASCs retained their stemness. Cells were cultured in the appropriate differentiation medium; they were then stained for Alizarin Red which identifies calcium deposits indicative of functional osteocytes or Oil Red which stains cytoplasmic lipid droplets of adipocytes. The results showed that Venus+ASCs can efficiently differentiate towards osteogenic and adipogenic cell lineages (Fig. 1E). It was thus confirmed that Venus+ASCs retained their stemness and differentiation potential, in accordance with previously established criteria (Dominici et al., 2006).

Spatial distribution of Venus+ASCs

At 7dPI, numerous transplanted ASCs were detected within the host brains, strongly expressing the Venus fluorescent protein. The majority of Venus+ASCs had migrated into the periventricular parenchyma and were localized within the SVZ and throughout the adjacent striatal grey matter. These cells were multipolar in shape, extending thick processes (Fig. 2). Only few Venus+ ASCs were detected within the ventricular infusion site, attached to the ependymal wall, some of them invading the subependymal layer of the brain parenchyma. Occasionally, Venus+ASCs were observed in the corpus callosum or the septum, at the level of the lateral ventricle in sections where the needle insertion traces were visible. Transplanted cells were not observed along white matter migratory pathways or at the injury site. There were no differences in the spatial distribution or extent of migration between TBI+ASCs and naive+ASCs animals.

We further sought to examine whether Venus+ASCs differentiated towards neuronal or glial lineages after transplantation. Immunohistochemical analysis showed that these cells did not express the lineage differentiation markers GFAP, S100, NeuN, DCX or calbindin, suggesting that they retained their mesenchymal nature *in vivo*.

Host brain responses to transplantation of Venus+ASCs

Effects of Venus+ASCs on the periventricular striatal parenchyma

In order to characterize the brain microenvironment where the vast majority of Venus+ASCs were localized, we performed immunocytochemical labelling for GFAP, Iba, Ki67 and vWF, as well as histological M TRI, on sections taken at the level of the lateral ventricle and containing the striatum. The striatal parenchyma displayed aggregations of intensely stained GFAP+ astrocytes, emanating thick processes that contributed to a dense network surrounding Venus+ASCs cells, both in TBI+ASCs and in naive+ASCs animals, whereas in the TBI+saline group, GFAP+ astrocytes were smaller, had thinner processes and were evenly scattered throughout the striatal grey matter (Fig. 2A-C). Quantification of GFAP staining intensity, estimated as pixel area/optical field, showed that it was significantly higher after transplantation, compared to TBI alone (Fig. 2L). Additionally, Venus+ASCs were embedded among numerous Iba+ microglia mainly in TBI+ASCs but also in naive+ASCs animals, which exhibited a ramified morphology, whereas in TBI+saline animals the striatum

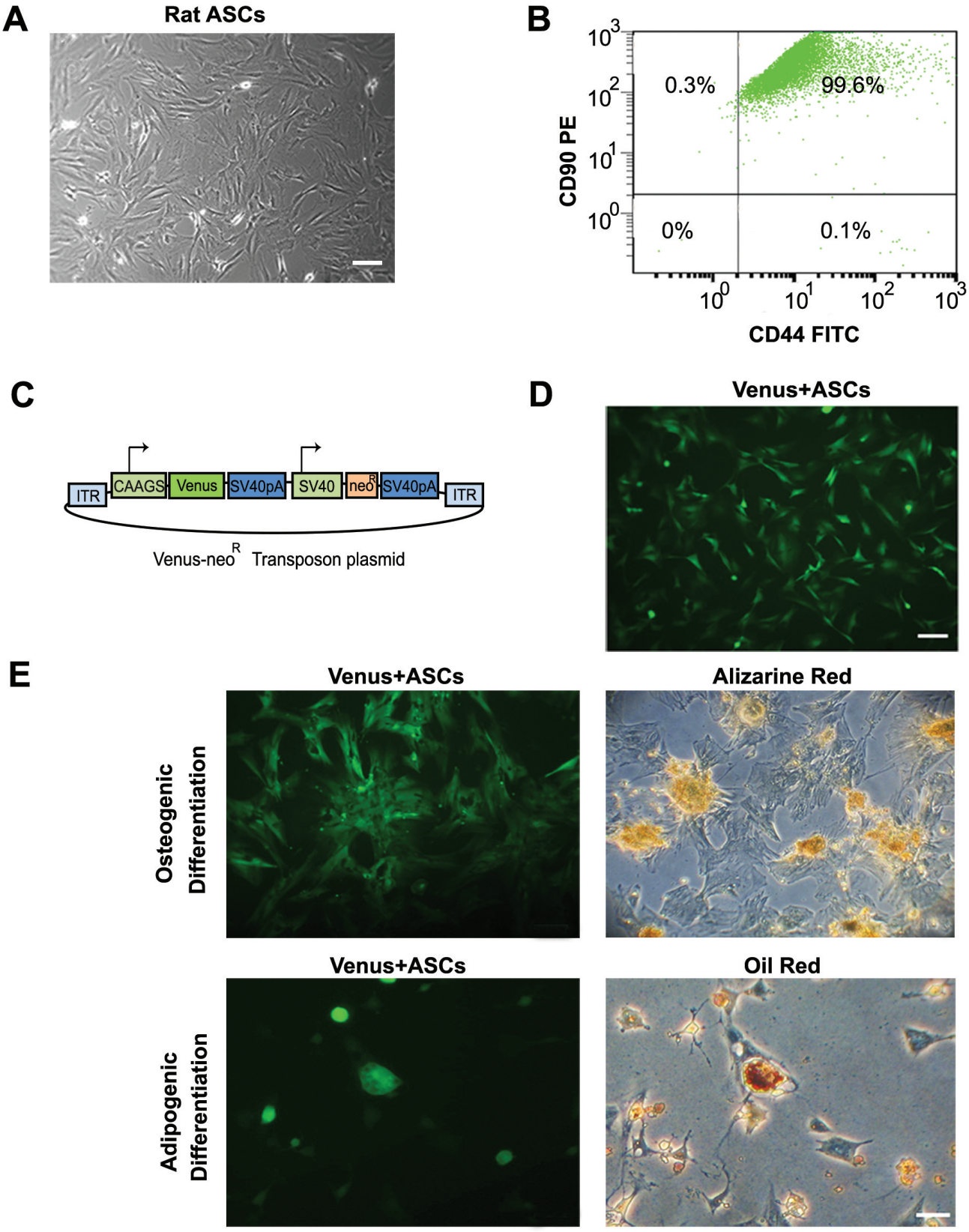

Fig. 1. Generation and characterization of Venus+ASCs. **A.** Phase contrast images of ASCs culture. **B.** Flow cytometry of ASCs for CD44 and CD90 mesenchymal stromal-cell markers. **C.** Schematic representation of a Venus-neoR transposon, used to genetically label ASCs. **D.** Fluorescence microscopy of Venus+ASCs. **E.** Multilineage differentiation of Venus+ASCs towards osteocytes or adipocytes, revealed by Alizarin Red or Oil Red staining, respectively. Scale bars: A, D, 100 µm; E, 50 µm.

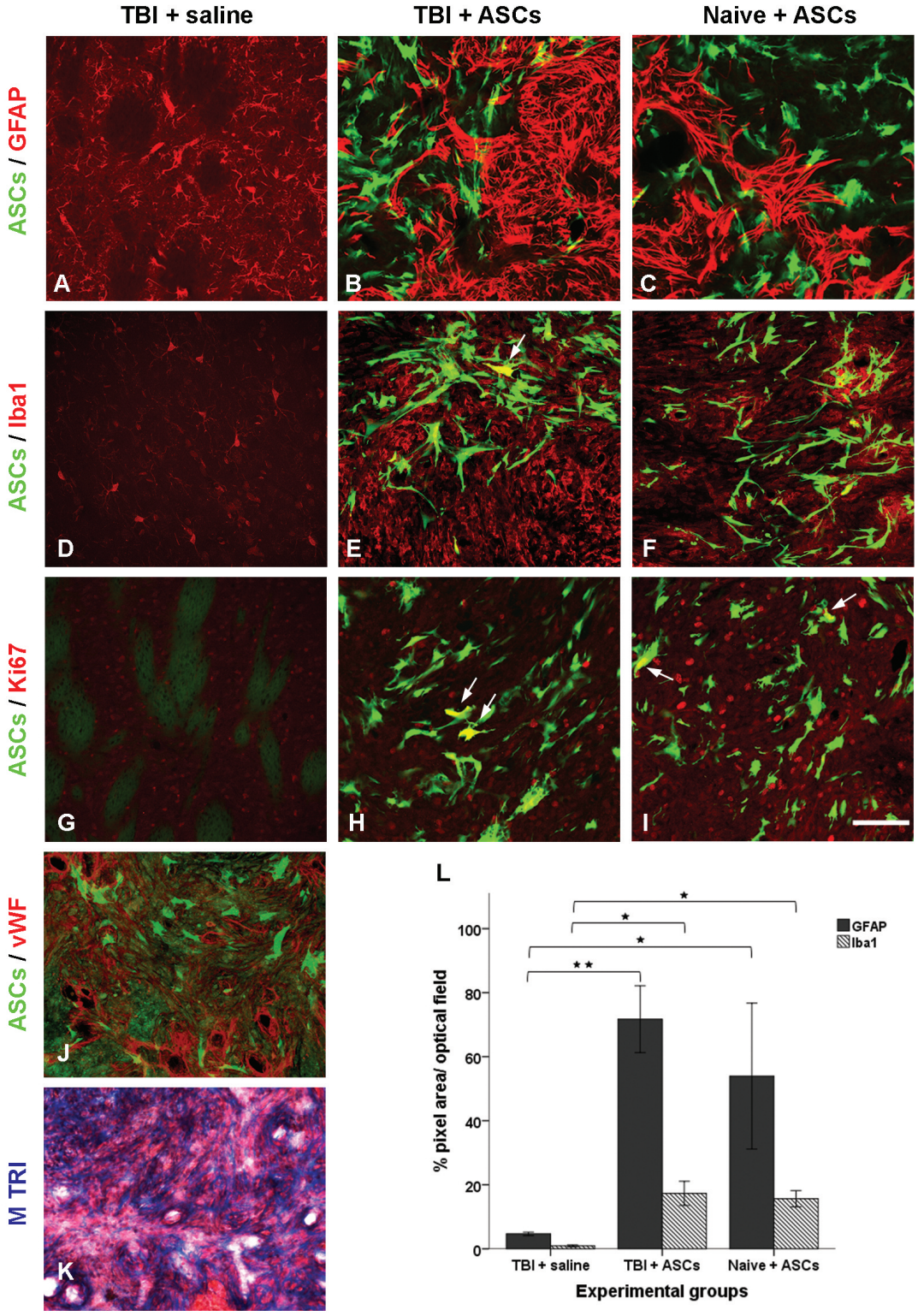

Fig. 2. Effects of Venus+ASCs on the striatal parenchyma. Confocal micrographs of sections containing Venus+ASCs and immunostained for GFAP **(A-C)**, Iba1 **(D-F)**, Ki67 **(G-I)** and vWF **(J)**, and photomicrograph of section processed for M TRI **(K)**. In TBI+ASCs and naive+ASCs animals, Venus+ASCs are surrounded by dense aggregations of GFAP+ astrocytes **(B, C)**, Iba+microglia **(E, F)** and Ki67+proliferating cells **(H, I)**, whereas TBI+saline animals display a sparse distribution of immunoreactive cells **(A, D, G)**. Arrows point at double labelled cells for Venus and Iba1 **(E)**, Venus and Ki67 **(H, I)**. In TBI+ASCs animals, Venus+ASCs are in close proximity with the vWF+endothelial wall of striatal blood vessels **(J)**, whilst M TRI reveals dense labelling for collagen depositions within the striatum **(K)**. **L.** Histogram shows significant differences in the expression of GFAP and Iba1 in the striatum, between transplanted and non-transplanted animals. * P<0.05: naive+ASCs versus TBI+saline (GFAP); TBI+ASCs versus TBI+saline (Iba1); naive+ASCs versus TBI+saline (Iba1); **P<0.001: TBI+ASCs versus TBI+saline (GFAP). Data are mean ±SD (n=6 for each experimental group). Scale bar: 100 μm.

displayed a markedly lower number and sparse distribution of Iba+ cells, with few thin processes (Fig. 2D-F). Quantification of Iba staining intensity showed that it was significantly higher after transplantation, compared to TBI alone (Fig. 2L). Co-localization of the Venus signal with Iba was rarely noted. Venus+ASCs were also intermingled with Ki67+ cells, but only a small proportion of them co-expressed the proliferative marker Ki67 (Fig. 2H,I). In sections stained for vWF, Venus+ASCs cells surrounded or were in close proximity with the endothelial wall of striatal blood vessels (Fig. 2J). Finally, in sections processed for M TRI, dense collagen depositions were present throughout the striatal parenchyma only in animals that were subjected to transplantation (Fig. 2K). This finding indicates the production and deposition of collagen fibres in the striatal extracellular matrix by Venus+ASCs.

Effects of Venus+ASCs on neurogenic niches

With the aim of investigating the effects of Venus+ASCs on host brain neurogenesis, we quantified the newly-produced NSCs in the neurogenic niches of the adult brain, the SVZ and the hippocampal DG. The BrdU-injection protocol allows for the visualization of $BrdU^+$ cells, which are mainly rapidly dividing NSCs within the niches.

Quantitative analysis in the SVZ revealed that Venus+ASCs significantly increased the absolute number of $BrdU^+$ cells in the ipsilateral hemisphere, compared to the effect of TBI (Fig. 3A-C,G). Transplantation increased the absolute number of $BrdU^+$ cells also in the contralateral hemisphere, but this increase was not significant, compared to TBI alone (Fig. 4G).

Quantitative analysis in the hippocampal DG revealed that, similarly to SVZ, after transplantation, the absolute number of BrdU + cells in the ipsilateral hemisphere was significantly higher, compared to TBI alone (Fig. 3D-F, H). Transplantation increased the absolute number of BrdU + cells also in the contralateral hemisphere, but this increase was significant only for the TBI+ASCs animal group (Fig. 3H).

Effects of Venus+ASCs on the cortical injury site

Quantification of the volume of the injury-induced cortical cavity showed that it was significantly reduced after transplantation, compared to TBI alone (TBI+ASCs: 16.55±4.35; TBI+saline: 26.84±5.67, $P<0.05$), (Fig. 4A-C).

The effect of Venus+ASCs transplantation on the astrocytic and the microglial/macrophage populations at the injury site was assessed with GFAP and Iba1 immunohistochemistry, respectively. In TBI+saline animals, a dense GFAP+ astroglial scar, consisting of thick, long and intertwined processes bordered the lesion core. The adjacent peri-lesion area was packed with GFAP+cells that displayed a large rounded soma with thick processes forming a dense network along with scar-originating processes. In contrast, injured brains that received transplantation, showed notable alterations in the morphology of GFAP+ cells, mainly in the perilesion area. Labelled cells had acquired a star-like shape emanating thinner, ramified, and not intermingled processes. In naive+ASCs animals, GFAP+ cells were small, with thin processes and sparsely distributed in the corresponding brain area (Fig. 4D-F). Quantification of GFAP staining intensity, estimated as pixel area/optical field, showed that it did not differ markedly between TBI+saline and TBI+ASCs animal groups, but was significantly higher in both groups compared to naive+ASCs animals (Fig. 4J).

Quantification of Iba1+ cells revealed that the number of microglia/macrophages in the core-surrounding peri-lesion area did not differ markedly between the TBI+ASCs and TBI+saline groups, but was significantly higher in both animal groups that were subjected to TBI, compared to naive+ASCs animals (Fig. 4K). The expression of Iba1, quantified as pixel area/optical field, was significantly upregulated in both transplanted and non-transplanted groups subjected to TBI, compared to naive+ASCs animals. Additionally, after TBI, the expression of Iba1 was significantly higher in the presence of transplanted cells (Fig. 4J). This suggests that TBI mobilized microglia/macrophages in the peri-lesion area, whereas transplantation had no effect on their number, but increased Iba1 expression. Notably, Venus+ASCs induced marked changes in the morphological features of the microglial population. Iba1+ cells exhibited mainly an amoeboid or rounded shape with thick, short and unbranched processes in TBI+saline animals, whereas they were mostly multipolar, with thin and extensively ramified processes in TBI+ASCs animals. In naive+ASCs animals, Iba+ cells were sparse and had a small soma with thin processes (Fig. 4G-I).

Discussion

The present results demonstrate that genetically labelled Venus+ASCs, 1) survive at least for seven days in the rat brain parenchyma and migrate from the ventricular infusion site into the periventricular striatal parenchyma; 2) do not differentiate during the observation time frame towards neuronal or glial lineages, but retain their mesenchymal nature; and 3) are capable of modifying the host brain's cellular response to injury.

Survival, migration and differentiation of Venus+ASCs

Our first goal was to examine the survival, migration and differentiation of Venus+ASCs administered into the ipsilateral lateral ventricle directly after TBI. The present results demonstrate that Venus+ASCs were able to survive and migrate into the adjacent striatum, where

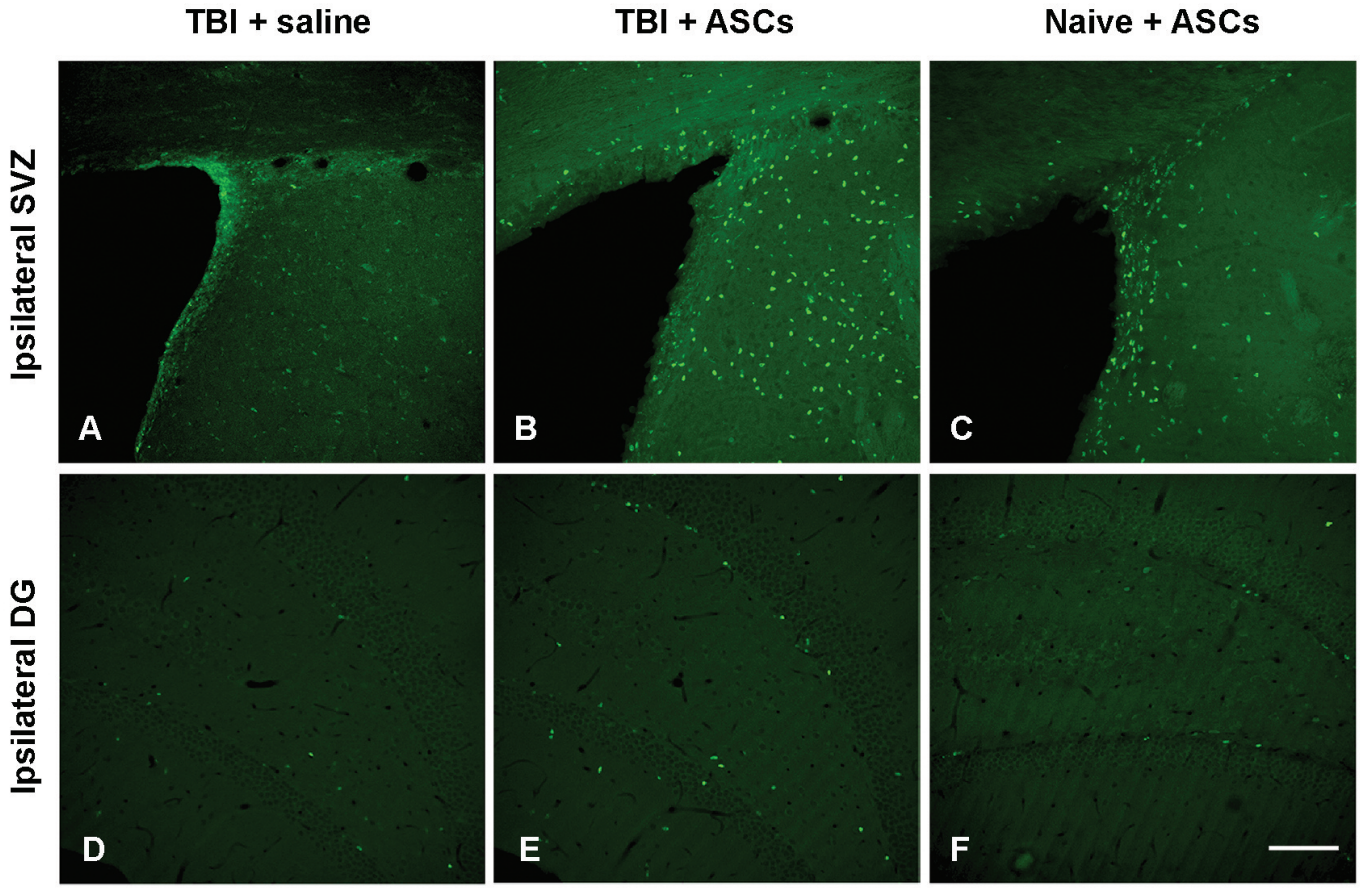

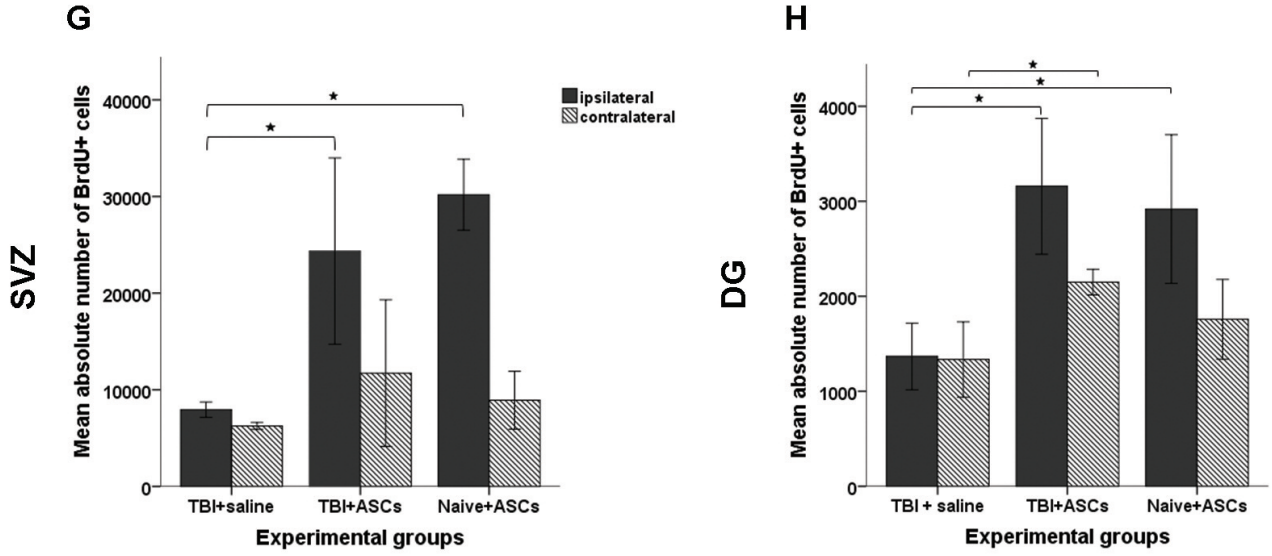

Fig. 3. Venus+ASCs stimulate the production of NSCs in neurogenic niches. **A, D.** In the ipsilateral SVZ and hippocampal DG, the mean absolute number of BrdU+cells after TBI alone is significantly lower than that induced by transplantation in the presence **(B, E)** or absence **(C, F)** of injury. Histograms show significant differences between animals subjected only to TBI and animals that received transplantation, in the SVZ **(G)** and the hippocampal DG **(H)**. * P<0.05: **(G)** TBI+ASCs versus TBI+saline; naive+ASCs versus TBI+saline (ipsilateral); **(H)** TBI+ASCs versus TBI+saline (ipsilateral; and contralateral); naive+ASCs versus TBI+saline (ipsilateral). Data are mean ±SD (n=6 for each experimental group). Scale bar: 100 µm.

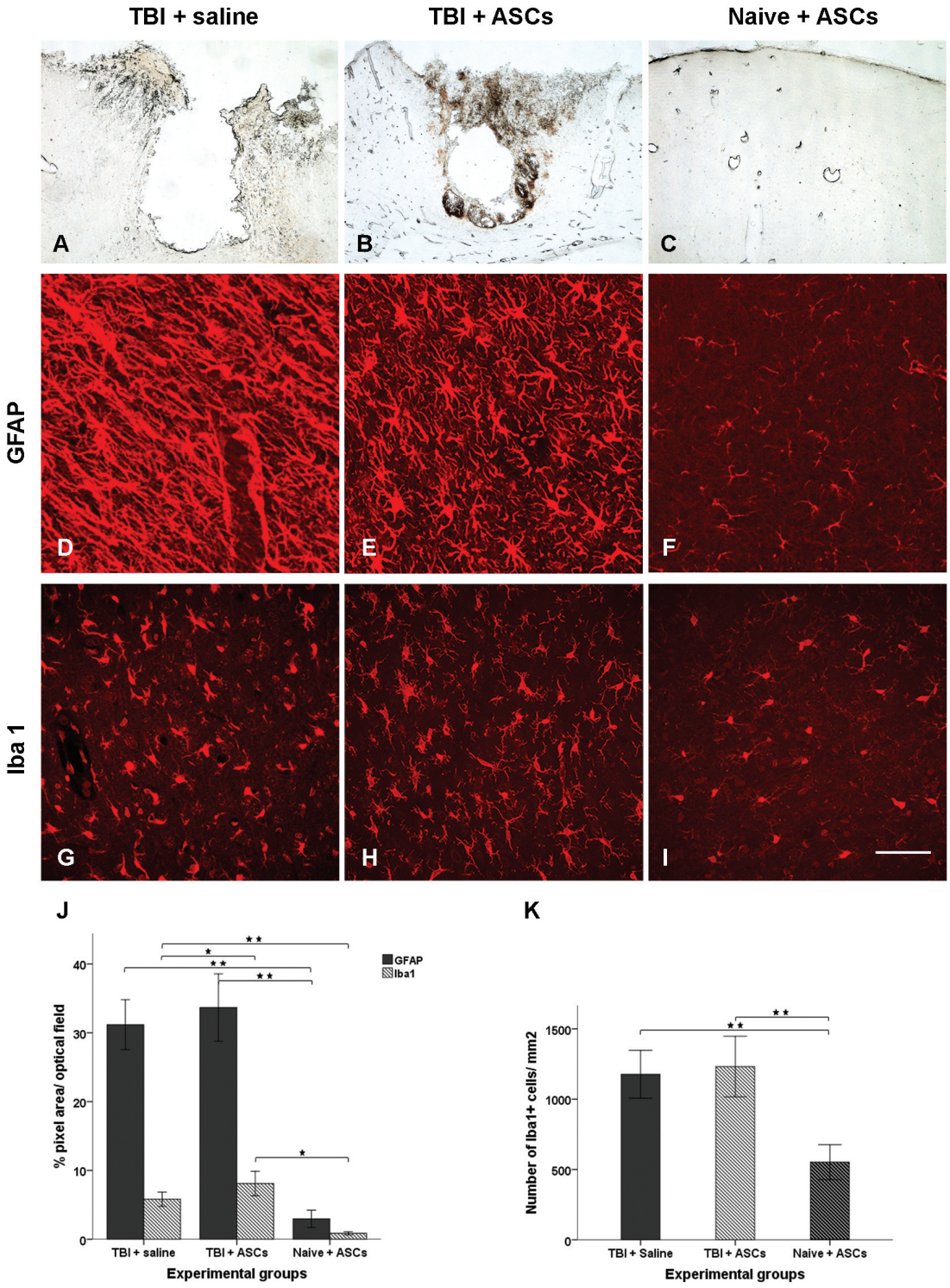

Fig. 4. Effects of Venus+ASCs on the cortical injury site. Transplantation of Venus+ASCs decreases the TBI-induced lesion area and induces marked changes in the morphology of the Iba1+ microglia and GFAP+ astrocytes in the perilesion area. **A-C.** Photomicrographs of coronal sections containing the cortical cavity of TBI+saline, TBI+ASCs animals and the corresponding cortical area in naïve+ASCs animals, respectively. Confocal micrographs show the morphology of GFAP+ astrocytes **(D-F)** and Iba1+ microglia **(G-I)** in the cortical perilesion area. In TBI+saline animals, GFAP+ astrocytes are rounded with thick, intermingled processes **(D)**, whereas in TBI+ASCs animals they are star-shaped and ramified **(E)**. In naive+ASCs animals, they are small with thin processes and sparsely distributed **(F)**. In TBI+saline animals, Iba1+microglia have an amoeboid, unbranched morphology **(G)**, whereas in TBI+ASCs animals they are multipolar and extensively ramified **(H)**. In naive+ASCs animals, they are small with thin processes **(I)**. **J, K.** Histograms show significant differences in the expression of GFAP and Iba1 and in the number of Iba1+ cells in the cortical perilesion area. **(J)** * P<0.05: TBI+ASCs versus TBI+saline (Iba1); TBI+ASCs versus naive+ASCs (Iba1); **P<0.001: TBI+ASCs versus naive+ASCs (GFAP); TBI+saline versus naive+ASCs (GFAP); TBI+saline versus naive+ASCs (Iba1). (K) **P<0.001: TBI+ASCs versus naive+ASCs; TBI+saline versus naive+ASCs. Data are mean ±SD (n=6 for each experimental group). Scale bars: A-C, 400 μm; D-I, 100 μm.

they were confined at 7dPI and post-transplantation. At this stage, the migration of transplanted cells was not directed by the injury, as homing to the lesion site was not detected and their intrastriatal distribution pattern was similar in injured and uninjured brains. Immunohistochemical analysis showed that transplanted cells did not express the neuronal or glial lineage differentiation markers GFAP, DCX, S100, NeuN and calbindin. It has initially been assumed that the action of MSC is exerted through their differentiation potential into different lineages. However, strong evidence from *in vitro* and *in vivo* studies suggests that the properties of these cells are mediated by the secretion of soluble growth factors and cytokines in the extracellular space, as well as the involvement of their exosomes in cell-to-cell interactions (Teixeira et al., 2013). Moreover, it has been shown that phenotypic differentiation or migration of transplanted cells into the injury area is not essential for their effect on the recovery of brain functions (Shear et al., 2010).

Host brain responses to transplantation of Venus+ASCs

To gain insight into the host brain's responses to transplantation, we examined the two known adult neurogenic niches, the striatal cellular microenvironment of Venus+ASCs localization and the cortical injury site.

Effects of Venus+ASCs on neurogenic niches and the periventricular striatal parenchyma

In order to study the effects of Venus+ASCs on endogenous neurogenesis we quantified the newly produced NSCs in the SVZ and the hippocampal DG by estimating the absolute number of $BrdU^+$ cells in these areas. Our data demonstrate that transplantation induced a significant increase of the number of NSCs in both the SVZ and the hippocampal DG of the ipsilateral hemisphere, compared to the effect of TBI alone. These results are in line with previous reports suggesting that transplanted MSC interact with brain niches by stimulating neurogenesis (Munoz et al., 2005; Donega et al., 2014b; Teixeira et al., 2015). Studies on neonatal ischemic brain injury have shown that transplanted MSC do not differentiate into neurons or glial cells, suggesting that their action on damage restoration is exerted through the mobilization of endogenous NSCs, mediated by the secretion of neuroregulatory factors (van Velthoven et al., 2010; Donega et al., 2013b).

Considering evidence pointing towards the crucial role of the cellular microenvironment of the neurogenic niches in the production, survival migration and differentiation of neural stem/progenitor cells (Shen et al., 2004; Thored et al., 2009; Sierra et al., 2010; Culver et al., 2013), we performed a morphological, histological and immunohistochemical characterization of the periventricular striatal parenchyma where Venus+ASCs were localised, at the time point examined. We show that in the presence of transplanted cells, the striatum contained an abundance of Iba1+ microglia and Ki67+ proliferating cells, as well as dense accumulations of GFAP+ astrocytes, whereas after TBI alone, only a small number of sparsely distributed microglia, astrocytes and proliferating cells was noted. In addition, the staining intensity of Iba1 and GFAP was significantly higher in transplanted, compared to non-transplanted animals. The morphology of microglia and astrocytes also differed markedly between experimental groups. Different morphological phenotypes have previously been associated with different states of glial activation and distinct functional states (Colton, 2009; Chhor et al., 2013; Franco and Fernández-Suárez, 2015; Zanier et al., 2015). In the presence of Venus+ASCs, microglia exhibited an extensively ramified morphology which is similar to the reported anti-inflammatory phenotype that promotes neurogenesis in the adult rat SVZ after stroke (Thored et al., 2009). In contrast, after TBI alone, Iba1+ cells show moderate ramification features that presumably correspond to the resident brain microglia, which are considered as the active-surveyors of the attenuated M2 type (Davalos et al., 2005; Nimmerjahn et al., 2005; Franco and Fernández-Suárez, 2015; Zanier et al., 2015). In addition, after transplantation, the astrocytic population in this area aquired features such as increased staining intensity and dense aggregations of hypetrophic perikarya with thick intermingled processes, that signify astrocytic reactivity (Burda and Sofroniew 2014). It therefore appears that the production and activation of glial cells in this brain area which is remote to the injury site is stimulated only in the presence of transplanted cells.

Activated microglia have been suggested to regulate adult neurogenesis (Ziv et al., 2006; Cacci et al., 2008). Microglial activation with an anti-inflammatory profile in the striatum has been proposed to promote neurogenesis in the SVZ of rat stroke models (Thored et al., 2009). A distinct population of microglia has recently been identified in the SVZ that promotes survival and migration of neural progenitor cells (Ribeiro Xavier et al., 2015). Considering that a co-expression of Iba+ with Venus+ was only rarely noted, we suggest that transplantation-activated microglia in the striatum are not involved in the phagocytosis of Venus+ASCs but may rather contribute to neurogenic processes in the neighboring SVZ niche. It is also known that niche-localized reactive astrocytes provide structural support for proliferating cells, secrete factors that sustain neurogenesis, guide the migration of neuroblasts and control the functional integration of adult-born hippocampal neurons (Ehret et al., 2015; Platel and Bordey, 2015; Sultan et al., 2016).

The data of the present study also indicated that Venus+ASCs were associated with the endothelial cells of striatal microvasculature. *In vitro* and *in vivo* studies have shown angiogenic properties of human ASCs, which are implicated in tissue regeneration (Kingham et al., 2014). The microvasculature of the SVZ and the hippocampus has been shown to modulate the

proliferation and migration of NSCs by means of endothelial secretion of soluble factors (Gómez-Gaviro et al., 2012; Delgado et al., 2014). In conjunction with this evidence, our data suggest that enhanced neurogenesis in the injured brain is mediated by an interplay between transplanted Venus+ASCs and the local cellular microenvironment.

Apart from the existing hypotheses concerning the action of MSC through trophic or cell-to-cell interactions, a novel mode of action was lately put forward, according to which these cells form a metalloproteinases-rich biobridge between the area of cortical injury and the SVZ that may serve for directing migration of newly produced cells (Tajiri et al., 2014b). Extracellular-matrix molecules are believed to be involved in plasticity and regeneration after CNS damage (Jakeman et al., 2014; Fawcett, 2015). In the present study, collagen depositions were detected throughout the striatum in transplanted animals, but were not observed after TBI alone. This provides further evidence that the mesenchymal identity of transplanted Venus+ASCs persists *in vivo*. Whether Venus+ASCs-produced collagen depositions in the extracellular matrix provide a permissive or inhibitory substrate for reparative processes remains to be elucidated.

Effects of Venus+ASCs on the cortical injury site

Our data indicate that Venus+ASCs were capable of modifying the host brain's response also at the injury site. Transplantation promoted wound healing through the significant reduction of the injury volume, in agreement with previous reports (Kaengkan et al., 2013; Tajiri et al., 2014a). Venus+ASCs did not affect the number of TBI-activated microglia/macrophages, but induced profound changes in their morphology. After TBI, microglia/macrophages displayed an amoeboid unbranched morphology that has been associated with the classically activated M1 phenotype with pro-inflammatory functions. In contrast, following transplantation, these cells acquired an enlarged and extensively ramified morphology that correlates well to the alternatively activated M2 phenotype with anti-inflammatory actions, involved in tissue repair, regeneration and immunomodulation (Colton, 2009; Chhor et al., 2013; Franco and Fernández-Suárez, 2015; Velázquez et al., 2015; Zanier et al., 2015; Loane and Kumar, 2016). This is confirmed by our quantitative analysis that shows an increase of Iba1+ pixel area in the cortical injury site, without a concomitant increase in the number of Iba+ cells. Additionally, transplantation of Venus+ASCs did not affect the staining intensity of the TBI-induced glial scar, but considerably modified the morphology of the astrocytic population, mainly at the cortical peri-injury site, from the characteristic hypertrophic reactive phenotype to a star-like ramified type. Taken together, the present results suggest that Venus+ASCs are capable not only of modifying the cellular microenvironment at their localization site, but also of inducing morphological changes that may reflect different functional states of reactive gliosis in the remote brain injury site. This implies that their actions at the cortical area are exerted through paracrine mechanisms.

It has been suggested that functions of reactive glial cells after brain damage are modulated by differential molecular signalling mechanisms regulating synaptic plasticity and neural remodelling (Burda and Sofroniew, 2014; Burda et al., 2016). Our data are consistent with previous *in vivo* and *in vitro* studies which showed that MSC can shift the inflammatory environment of the injured brain to a regeneration-permissive state, through the early polarization of microglia/macrophages towards the M2 phenotype (Donega et al., 2014a; Hegyi et al., 2014; Zanier et al., 2014). ASCs co-cultured with microglia have been shown to reverse their inflammatory phenotype into an alternative anti-inflammatory, neurotrophic one, both in the presence and in the absence of inflammation, by the secretion of trophic factors (Neubrand et al., 2014). Our results, in conjunction with these reports, may imply a transplantation-induced reprogramming of the glial state from a detrimental pro-inflammatory to a beneficial anti-inflammatory one that promotes tissue repair after injury. Considering that eliminating long-lasting neuroinflammation is a prerequisite for structural and functional recovery, ASCs may be promising tools for interventions that aim at modifying the microenvironment of the lesion site without eliminating the protective function of the glial scar, but achieving the optimal balance of glial polarization for brain repair.

Conclusions

The present results indicate that genetically labelled ASCs promote reparative/regenerative processes in the injured brain which are not mediated by homing to the injury site or differentiation towards neuronal/glial lineages, but rather through the modulation of the neuroinflammatory response and the enhancement of neurogenic processes. We suggest that the genetic manipulation required for this labelling does not affect the impact of ASCs on injury resolution. The method used here could pave the way for the production and implementation of stem cell lines, engineered to produce neuroprotective factors or molecules that are down-regulated after injury. This approach could use the beneficial effects of gene and stem cell therapy for the development of novel therapeutic strategies aiming at the functional restoration of the injured brain.

Acknowledgements. We thank M. Chiotelli for technical assistance. This work was supported by the Research Committee of Aristotle University of Thessaloniki and Biohellenika. Authors wish to thank Dr. Z. Ivics and Dr. Z. Izsvák for kindly providing the Sleeping Beauty 100X transposon system.

References

Bekiari C., Giannakopoulou A., Siskos N., Grivas I., Tsingotjidou A., Michaloudi H. and Papadopoulos G.C. (2015). Neurogenesis in the septal and temporal part of the adult rat dentate gyrus. Hippocampus 25, 511-523.

Burda J.E. and Sofroniew M.V. (2014). Reactive gliosis and the multicellular response to CNS damage and disease. Neuron 81, 229-248.

Burda J.E., Bernstein A.M. and Sofroniew M.V. (2016). Astrocyte roles in traumatic brain injury. Exp. Neurol. 275, 305-315.

Cacci E., Ajmone-Cat M.A., Anelli T., Biagioni S. and Minghetti L. (2008). *In vitro* neuronal and glial differentiation from embryonic or adult neural precursor cells are differently affected by chronic or acute activation of microglia. Glia 56, 412-425.

Cameron H.A. and Mckay R.D.G. (2001). Adult neurogenesis produces a large pool of new granule cells in the dentate gyrus. J. Comp. Neurol. 435, 406-417.

Chhor V., Le Charpentier T., Lebon S., Oré M.V., Celador I.L., Josserand J., Degos V., Jacotot E., Hagberg H., Sävman K., Mallard C., Gressens P. and Fleiss B. (2013). Characterization of phenotype markers and neuronotoxic potential of polarised primary microglia *In vitro*. Brain Behav. Immun. 32, 70-85.

Chung T.N., Kim J.H., Choi B.Y., Chung S.P., Kwon S.W. and Suh S.W. (2015). Adipose-derived mesenchymal stem cells reduce neuronal death after transient global cerebral ischemia through prevention of blood-brain barrier disruption and endothelial damage. Stem Cells Transl. Med. 4 , 178-185.

Colton C.A. (2009). Heterogeneity of microglial activation in the innate immune response in the brain. J. Neuroimmune Pharmacol. 4, 399-418.

Constantin G., Marconi S., Rossi B., Angiari S., Calderan L., Anghileri E., Gini B., Bach S.D., Martinello M., Bifari F., Galiè M., Turano E., Budui S., Sbarbati A., Krampera M. and Bonetti B. (2009). Adipose-derived mesenchymal stem cells ameliorate chronic experimental autoimmune encephalomyelitis. Stem Cells 27, 2624-2635.

Culver J.C., Vadakkan T.J. and Dickinson M.E. (2013). A specialized microvascular domain in the mouse neural stem cell niche. PLoS One 8, e53546.

Davalos D., Grutzendler J., Yang G., Kim J.V, Zuo Y., Jung S., Littman D.R., Dustin M.L. and Gan W.-B. (2005). ATP mediates rapid microglial response to local brain injury *in vivo*. Nat. Neurosci. 8, 752-758.

Delgado A.C., Ferrón S.R., Vicente D., Porlan E., Perez-Villalba A., Trujillo C.M., D'Ocón P. and Fariñas I. (2014). Endothelial NT-3 delivered by vasculature and CSF promotes quiescence of subependymal neural stem cells through nitric oxide induction. Neuron 83, 572-585.

Díez-Tejedor E., Gutiérrez-Fernández M., Martínez-Sánchez P., Rodríguez-Frutos B., Ruiz-Ares G., Lara M.L. and Gimeno B.F. (2016). Reparative therapy for acute ischemic stroke with allogeneic mesenchymal stem cells from adipose tissue: A safety assessment. J. Stroke Cerebrovasc. Dis. 23, 2694-2700.

Dominici M., Le Blanc K., Mueller I., Slaper-Cortenbach I., Marini F., Krause D., Deans R., Keating A., Prockop D. and Horwitz E. (2006). Minimal criteria for defining multipotent mesenchymal stromal cells. The International Society for Cellular Therapy position statement. Cytotherapy 8, 315-317.

Donega V., Nijboer C.H., Braccioli L., Slaper-Cortenbach I., Kavelaars A., Van Bel F. and Heijnen C.J. (2014a). Intranasal administration of human MSC for ischemic brain injury in the mouse: *In vitro* and *in vivo* neuroregenerative functions. PLoS One 9, e112339.

Donega V., Nijboer C.H., van Tilborg G., Dijkhuizen R.M., Kavelaars A. and Heijnen C.J. (2014b). Intranasally administered mesenchymal stem cells promote a regenerative niche for repair of neonatal ischemic brain injury. Exp. Neurol. 261, 53-64.

Donega V., van Velthoven C.T.J., Nijboer C.H., Kavelaars A. and Heijnen C.J. (2013a). The endogenous regenerative capacity of the damaged newborn brain: boosting neurogenesis with mesenchymal stem cell treatment. J. Cereb. Blood Flow Metab. 33, 625-634.

Donega V., van Velthoven C.T.J., Nijboer C.H., van Bel F., Kas M.J.H., Kavelaars A. and Heijnen C.J. (2013b). Intranasal mesenchymal stem cell treatment for neonatal brain damage: long-term cognitive and sensorimotor improvement. PLoS One 8, e51253.

Ehret F., Vogler S. and Kempermann G. (2015). A co-culture model of the hippocampal neurogenic niche reveals differential effects of astrocytes, endothelial cells and pericytes on proliferation and differentiation of adult murine precursor cells. Stem Cell Res. 15, 514-521.

Fawcett J.W. (2015). The extracellular matrix in plasticity and regeneration after CNS injury and neurodegenerative disease. Prog. Brain Res. 218, 213-226.

Franco R. and Fernández-Suárez D. (2015). Alternatively activated microglia and macrophages in the central nervous system. Prog. Neurobiol. 131, 65-86.

Gennai S., Monsel A., Hao Q., Liu J., Gudapati V., Barbier E.L. and Lee J.W. (2015). Cell-based therapy for traumatic brain injury. Br. J. Anaesth. 115, 203-212.

Gimble J.M., Guilak F. and Bunnell B.A. (2010). Clinical and preclinical translation of cell-based therapies using adipose tissue-derived cells. Stem Cell Res. Ther. 1, 19.

Gómez-Gaviro M.V., Scott C.E., Sesay A.K., Matheu A., Booth S., Galichet C. and Lovell-Badge R. (2012). Betacellulin promotes cell proliferation in the neural stem cell niche and stimulates neurogenesis. Proc. Natl. Acad. Sci. USA 109, 1317-1322.

Hegyi B., Környei Z., Ferenczi S., Fekete R., Kudlik G., Kovács K.J., Madarász E. and Uher F. (2014). Regulation of mouse microglia activation and effector functions by bone marrow-derived mesenchymal stem cells. Stem Cells Dev. 23, 2600-2612.

Jakeman L.B., Williams K.E. and Brautigam B. (2014). In the presence of danger: The extracellular matrix defensive response to central nervous system injury. Neural Regener. Res. 9, 377-384.

Jumabay M. and Boström K.I. (2015). Dedifferentiated fat cells: A cell source for regenerative medicine. World J. Stem Cells 7, 1202.

Kaengkan P., Baek S.E., Kim J.Y., Kam K.Y., Do B.R., Lee E.S. and Kang S.G. (2013). Administration of mesenchymal stem cells and ziprasidone enhanced amelioration of ischemic brain damage in rats. Mol. Cells 36, 534-541.

Kalbermatten D.F., Schaakxs D., Kingham P.J. and Wiberg M. (2011). Neurotrophic activity of human adipose stem cells isolated from deep and superficial layers of abdominal fat. Cell Tissue Res. 344, 251-260.

Kapur S.K. and Katz A.J. (2013). Review of the adipose derived stem cell secretome. Biochimie 95, 2222-2228.

Karathanasis V., Petrakis S., Topouridou K., Koliakou E., Koliakos G. and Demiri E. (2013). Intradermal injection of GFP-producing adipose stromal cells promotes survival of random-pattern skin flaps in rats. Eur. J. Plast. Surg. 36, 281-288.

Kernie S.G. and Parent J.M. (2010). Forebrain neurogenesis after focal ishcemic and traumatic brain injury. Neurobiol. Dis. 37, 267-274.

Kingham P.J., Kolar M.K., Novikova L.N., Novikov L.N. and Wiberg M. (2014). Stimulating the neurotrophic and angiogenic properties of human adipose-derived stem cells enhances nerve repair. Stem Cells Dev. 23, 741-54.

Kronenberg G., Reuter K., Steiner B., Brandt M.D., Jessberger S., Yamaguchi M. and Kempermann G. (2003). Subpopulations of proliferating cells of the adult hippocampus respond differently to physiologic neurogenic stimuli. J. Comp. Neurol. 467, 455-463.

Kumar A., Alvarez-Croda D.-M., Stoica B.A., Faden A.I. and Loane D.J. (2016). Microglial/Macrophage polarization dynamics following traumatic brain injury. J. Neurotrauma 33, 1732-1750.

Loane D.J. and Kumar A. (2016). Microglia in the TBI brain: The good, the bad, and the dysregulated. Exp. Neurol. 275, 316-327.

Mastro-Martínez I., Pérez-Suárez E., Melen G., González-Murillo Á., Casco F., Lozano-Carbonero N., Gutiérrez-Fernández M., Díez-Tejedor E., Casado-Flores J., Ramírez-Orellana M. and Serrano-González A. (2015). Effects of local administration of allogenic adipose tissue-derived mesenchymal stem cells on functional recovery in experimental traumatic brain injury. Brain Inj. 29, 1497-1510.

Mates L., Chuah M.K.L., Belay E., Jerchow B., Manoj N., Acosta-Sanchez A., Grzela D.P., Schmitt A., Becker K., Matrai J., Ma L., Samara-Kuko E., Gysemans C., Pryputniewicz D., Miskey C., Fletcher B., VandenDriessche T., Ivics Z. and Izsvak Z. (2009). Molecular evolution of a novel hyperactive Sleeping Beauty transposase enables robust stable gene transfer in vertebrates. Nat. Genet. 41, 753-761.

McDonald H.Y. and Wojtowicz J.M. (2005). Dynamics of neurogenesis in the dentate gyrus of adult rats. Neurosci. Lett. 385, 70-75.

Mellios K., Zacharaki T., Sophou S., Latsari M., Antonopoulos J., Dinopoulos A., Parnavelas J.G. and Dori I. (2009). Natural and lesion-induced apoptosis in the rat striatum during development. Brain Res. 1252, 30-44.

Munoz J.R., Stoutenger B.R., Robinson A.P., Spees J.L. and Prockop D.J. (2005). Human stem/progenitor cells from bone marrow promote neurogenesis of endogenous neural stem cells in the hippocampus of mice. Proc. Natl. Acad. Sci. USA 102, 18171-18176.

Murohara T., Shintani S. and Kondo K. (2009). Autologous adipose-derived regenerative cells for therapeutic angiogenesis. Curr. Pharm. Des. 15, 2784-2790.

Neubrand V.E., Pedreño M., Caro M., Forte-Lago I., Delgado M. and Gonzalez-Rey E. (2014). Mesenchymal stem cells induce the ramification of microglia via the small RhoGTPases Cdc42 and Rac1. Glia 62, 1932-1942.

Nimmerjahn A., Kirchhoff F. and Helmchen F. (2005). Resting microglial cells are highly dynamic surveillants of brain parenchyma *in vivo*. Science 308, 1314-1318.

Paxinos G. and Watson C. (2013). The rat brain in stereotaxic coordinates. 7th ed. Elsevier. Academic Press. Oxford. pp 1-472.

Petrakis S., Raskó T., Mátés L., Ivics Z., Izsvák Z., Kouzi-Koliakou K. and Koliakos G. (2012). Gateway-compatible transposon vector to genetically modify human embryonic kidney and adipose-derived stromal cells. Biotechnol. J. 7, 891-897.

Platel J.C. and Bordey A. (2015). The multifaceted subventricular zone astrocyte: From a metabolic and pro-neurogenic role to acting as a neural stem cell. Neuroscience 323, 20-28.

Ra J.C., Shin I.S., Kim S.H., Kang S.K., Kang B.C., Lee H.Y., Kim Y.J., Jo J.Y., Yoon E.J., Choi H.J. and Kwon E. (2011). Safety of intravenous infusion of human adipose tissue-derived mesenchymal stem cells in animals and humans. Stem Cells Dev. 20, 1297-1308.

Rehman J., Traktuev D., Li J., Merfeld-Clauss S., Temm-Grove C.J., Bovenkerk J.E., Pell C.L., Johnstone B.H., Considine R. V. and March K.L. (2004). Secretion of angiogenic and antiapoptotic factors by human adipose stromal cells. Circulation 109, 1292-1298.

Ribeiro Xavier A.L., Kress B.T., Goldman S.A., Lacerda de Menezes J.R. and Nedergaard M. (2015). A distinct population of microglia supports adult neurogenesis in the subventricular zone. J. Neurosci. 35, 11848-11861.

Rice A.C., Khaldi A., Harvey H.B., Salman N.J., White F., Fillmore H. and Bullock M.R. (2003). Proliferation and neuronal differentiation of mitotically active cells following traumatic brain injury. Exp. Neurol. 183, 406-417.

Richardson R.M., Singh A., Sun D., Fillmore H.L., Dietrich D.W. and Bullock M.R. (2009). Stem cell biology in traumatic brain injury: effects of injury and strategies for repair. J. Neurosurg. 112, 1125-1138.

Salgado A.J., Sousa J.C., Costa B.M., Pires A.O., Mateus-Pinheiro A., Teixeira F.G., Pinto L. and Sousa N. (2015). Mesenchymal stem cells secretome as a modulator of the neurogenic niche: basic insights and therapeutic opportunities. Front. Cell. Neurosci. 9, 249.

Schäffler A. and Büchler C. (2007). Concise review: adipose tissue-derived stromal cells--basic and clinical implications for novel cell-based therapies. Stem Cells 25, 818-827.

Shear D.A., Lu X.-C.M., Bombard M.C., Pedersen R., Chen Z., Davis A. and Tortella F.C. (2010). Longitudinal characterization of motor and cognitive deficits in a model of penetrating ballistic-like brain injury. J. Neurotrauma 27, 1911-1923.

Shen Q., Goderie S.K., Jin L., Karanth N., Sun Y., Abramova N., Vincent P., Pumiglia K. and Temple S. (2004). Endothelial cells stimulate self-renewal and expand neurogenesis of neural stem cells. Science 304, 1338-1340.

Sierra A., Encinas J.M., Deudero J.J.P., Chancey J.H., Enikolopov G., Overstreet-Wadiche L.S., Tsirka S.E. and Maletic-Savatic M. (2010). Microglia shape adult hippocampal neurogenesis through apoptosis-coupled phagocytosis. Cell Stem Cell 7, 483-495.

Sophou S., Dori I., Antonopoulos J., Parnavelas J.G. and Dinopoulos A. (2006). Apoptosis in the rat basal forebrain during development and following lesions of connections. Eur. J. Neurosci. 24, 573-585.

Sultan S., Li L., Moss J., Petrelli F., Cassé F., Gebara E., Lopatar J., Pfrieger F.W., Bezzi P., Bischofberger J. and Toni N. (2016). Synaptic integration of adult-born hippocampal neurons is locally controlled by astrocytes. Neuron 88, 957-972.

Sun D. (2016). Endogenous neurogenic cell response in the mature mammalian brain following traumatic injury. Exp. Neurol. 275, 405-410.

Tajiri N., Acosta S.A., Shahaduzzaman M., Ishikawa H., Shinozuka K., Pabon M., Hernandez-Ontiveros D., Kim D.W., Metcalf C., Staples M., Dailey T., Vasconcellos J., Franyuti G., Gould L., Patel N., Cooper D., Kaneko Y., Borlongan C.V and Bickford P.C. (2014a). Intravenous transplants of human adipose-derived stem cell protect the brain from traumatic brain injury-induced neurodegeneration and motor and cognitive impairments: cell graft biodistribution and soluble factors in young and aged rats. J. Neurosci. 34, 313-326.

Tajiri N., Duncan K., Antoine A., Pabon M., Acosta S.A., de la Pena I., Hernadez-Ontiveros D.G., Shinozuka K., Ishikawa H., Kaneko Y.,

Yankee E., McGrogan M., Case C. and Borlongan C.V. (2014b). Stem cell-paved biobridge facilitates neural repair in traumatic brain injury. Front. Syst. Neurosci. 8, 116.

Teixeira F.G., Carvalho M.M., Neves-Carvalho A., Panchalingam K.M., Behie L.A., Pinto L., Sousa N. and Salgado A.J. (2015). Secretome of mesenchymal progenitors from the umbilical cord acts as modulator of neural/glial proliferation and differentiation. Stem Cell Rev. 11, 288-297.

Teixeira F.G., Carvalho M.M., Sousa N. and Salgado A.J. (2013). Mesenchymal stem cells secretome: A new paradigm for central nervous system regeneration? Cell Mol. Life Sci. 70, 3871-3882.

Thored P., Heldmann U., Gomes-Leal W., Gisler R., Darsalia V., Taneera J., Nygren J.M., Jacobsen S.E., Ekdahl C.T., Kokaia Z. and Lindvall O. (2009). Long-term accumulation of microglia with proneurogenic phenotype concomitant with persistent neurogenesis in adult subventricular zone after stroke. Glia 57, 835-849.

Uccelli A., Laroni A. and Freedman M.S. (2011). Mesenchymal stem cells for the treatment of multiple sclerosis and other neurological diseases. Lancet Neurol. 10, 649-656.

Urrea C., Castellanos D.A., Sagen J., Tsoulfas P., Bramlett H.M. and Dietrich W.D. (2007). Widespread cellular proliferation and focal neurogenesis after traumatic brain injury in the rat. Restor. Neurol. Neurosci. 25, 65-76.

van Velthoven C.T.J., Kavelaars A., van Bel F. and Heijnen C.J. (2010). Repeated mesenchymal stem cell treatment after neonatal hypoxia-ischemia has distinct effects on formation and maturation of new neurons and oligodendrocytes leading to restoration of damage, corticospinal motor tract activity, and sensorimotor function. J. Neurosci. 30, 9603-9611.

Velázquez A., Ortega M., Rojas S., González-Oliván F.J. and Rodríguez-Baeza A. (2015). Widespread microglial activation in patients deceased from traumatic brain injury. Brain Inj. 9052, 1-8.

Villasana L.E., Kim K.N., Westbrook G.L. and Schnell E. (2015). Functional integration of adult-born hippocampal neurons after traumatic brain injury. eNeuro 2, 1-17.

Witcher K.G., Eiferman D.S. and Godbout J.P. (2015). Priming the inflammatory pump of the CNS after traumatic brain injury. Trends Neurosci. 38, 609-620.

Yañez R., Lamana M.L., García-Castro J., Colmenero I., Ramírez M. and Bueren J.A. (2006). Adipose tissue-derived mesenchymal stem cells have *in vivo* immunosuppressive properties applicable for the control of the graft-versus-host disease. Stem Cells 24, 2582-2591.

Zacharaki T., Sophou S., Giannakopoulou A., Dinopoulos A., Antonopoulos J., Parnavelas J.G. and Dori I. (2010). Natural and lesion-induced apoptosis in the dorsal lateral geniculate nucleus during development. Brain Res. 1344, 62-76.

Zanier E.R., Pischiutta F., Riganti L., Marchesi F., Turola E., Fumagalli S., Perego C., Parotto E., Vinci P., Veglianese P., D'Amico G., Verderio C. and De Simoni M.G. (2014). Bone marrow mesenchymal stromal cells drive protective M2 microglia polarization after brain trauma. neurotherapeutics 11, 679-695.

Zanier E.R., Fumagalli S., Perego C., Pischiutta F. and De Simoni M.-G. (2015). Shape descriptors of the "never resting" microglia in three different acute brain injury models in mice. Intensive Care Med Exp. 3, 1-18.

Zhang Y., Chopp M., Meng Y., Katakowski M., Xin H., Mahmood A. and Xiong Y. (2015). Effect of exosomes derived from multipluripotent mesenchymal stromal cells on functional recovery and neurovascular plasticity in rats after traumatic brain injury. J. Neurosurg. 122, 1-12.

Ziv Y., Ron N., Butovsky O., Landa G., Sudai E., Greenberg N., Cohen H., Kipnis J. and Schwartz M. (2006). Immune cells contribute to the maintenance of neurogenesis and spatial learning abilities in adulthood. Nat. Neurosci. 9, 268-275.

Accepted December 30, 2016